



Article

An In Vitro Study of the Antifungal Efficacy of Zinc Oxide Nanoparticles against Saccharomyces cerevisiae

Eng Pei Tan ¹, Sinouvassane Djearamane ^{1,*}, Ling Shing Wong ^{2,*}, Ranjithkumar Rajamani ³, Anto Cordelia Tanislaus Antony ^{4,*}, Suresh Kumar Subbaih ⁵, Ashok Kumar Janakiraman ⁶, Mohammod Aminuzzaman ^{4,7}, Vetriselvan Subramaniyan ⁸, Mahendran Sekar ⁹, and Siddharthan Selvaraj ¹⁰

- Department of Biomedical Science, Faculty of Science, Universiti Tunku Abdul Rahman, Kampar 31900, Malaysia
- ² Life Science Division, Faculty of Health and Life Sciences, INTI International University, Nilai 71800, Malaysia
- ³ Viyen Biotech LLP, Coimbatore 641031, India
- Department of Chemical Science, Faculty of Science, Universiti Tunku Abdul Rahman, Kampar 31900, Malaysia
- Centre for Materials Engineering and Regenerative Medicine, Bharath Institute of Higher Education and Research, Chennai 600126, India
- Department of Pharmaceutical Technology, Faculty of Pharmaceutical Sciences, USCI University, Kuala Lumpur 56000, Malaysia
- Centre for Photonics and Advanced Materials Research (CPAMR), Universiti Tunku Abdul Rahman (UTAR), Sungai Long Campus, Kajang 43000, Malaysia
- Faculty of Medicine, Bioscience and Nursing, MAHSA University, Kuala Lumpur 42610, Malaysia
- Department of Pharmaceutical Chemistry, Faculty of Pharmacy and Health Sciences, Royal College of Medicine Perak, Universiti Kuala Lumpur, Ipoh 30450, Malaysia
- Faculty of Dentistry, AIMST University, Bedong 08100, Malaysia
- * Correspondence: sinouvassane@utar.edu.my (S.D.); lingshing.wong@newinti.edu.my (L.S.W.); antoc@utar.edu.my (A.C.T.A.)

Abstract: Zinc oxide nanoparticles (ZnO NPs) are widely used in biomedical applications due to their antimicrobial and antioxidant properties. The objective of the present study was to determine the antifungal activity of ZnO NPs against the yeast *Saccharomyces cerevisiae*. The turbidity test results showed a significant (p < 0.05) dose-dependent growth inhibitory effect of ZnO NPs on *S. cerevisiae* as the growth inhibition increased from 7.04 ± 0.64 to $70.30 \pm 3.19\%$ as the concentration of ZnO NPs increased from 5 to 150 µg/mL. The scanning microscopy images evidenced the morphological alterations such as regional invagination, pitting, cracks, wrinkles, and cell wall rupture in the yeast cells treated with ZnO NPs. In addition, the FTIR spectrum revealed the possible involvement of hydroxyl, alkene, amides, carbonyl, and phosphate groups from polysaccharides, polypeptides, phospholipids, and ergosterol of the yeast cells wall for binding of ZnO NPs on the cell surface. The present study has demonstrated the antifungal activity of ZnO NPs on *S. cerevisiae* through growth inhibition and the morphological damages resulting from the treatment of ZnO NPs.

 $\textbf{Keywords:} \ yeast \ cells; \ growth \ inhibition; \ morphological \ alterations; \ scanning \ electron \ microscopy; \ FTIR$



Citation: Tan, E.P.; Djearamane, S.; Wong, L.S.; Rajamani, R.; Tanislaus Antony, A.C.; Subbaih, S.K.; Janakiraman, A.K.; Aminuzzaman, M.; Subramaniyan, V.; Sekar, M.; et al. An In Vitro Study of the Antifungal Efficacy of Zinc Oxide Nanoparticles against *Saccharomyces cerevisiae*.

Coatings 2022, 12, 1988. https://doi.org/10.3390/coatings12121988

Academic Editor: Anton Ficai

Received: 20 September 2022 Accepted: 17 November 2022 Published: 19 December 2022

Publisher's Note: MDPI stays neutral with regard to jurisdictional claims in published maps and institutional affiliations.



Copyright: © 2022 by the authors. Licensee MDPI, Basel, Switzerland. This article is an open access article distributed under the terms and conditions of the Creative Commons Attribution (CC BY) license (https://creativecommons.org/licenses/by/4.0/).

1. Introduction

Contagious diseases caused by fungi pose serious health threat to humans, and the incidence of fungal infections have been rising, despite the substantial progress achieved in the treatment and management of fungal infections [1]. Invasive fungal infections bring significant burden to healthcare systems with high morbidity and mortality rates, especially among immunocompromised patients, such as patients with Acquired Immune Deficiency Syndrome (AIDS), organ transplantation, or cancer patients with chemotherapy. The currently available major antifungal agents have limitations in terms of clinical efficacy and efficiency, resistance mechanisms, and toxicity of the compounds due to the similarities

Coatings **2022**, 12, 1988 2 of 12

between the fungi and human cells. Hence, it is of utmost importance to explore an alternative agent which not only fights against fungal infections but also prevents drug resistance [2–4].

Nanoscience and technology have played a vital role in the development of multiple fields ranging from engineering to biomedicine. Specifically, nanomaterials have been broadly applied in numerous industries due to their unique size- and shape-dependent physical, chemical, and biological properties [5–8]. Moreover, numerous metallic nanoparticles are widely believed to have antimicrobial properties against bacteria and fungi and also now used as surface coating materials in many medical devices to control the spread of infectious agents [9–11]. The usage of inorganic nanomaterials has attracted a considerable interest, owing primarily to their consistent antimicrobial activity on pathogenic microorganisms, which has been demonstrated to be effective even at low concentrations [12,13]. It is an emerging strategy to utilize the evolving nanoparticles as a base for successful treatment of infectious diseases by overcoming the antimicrobial resistance. Metal oxide nanoparticles, such as zinc oxide, silver, and titanium nanoparticles, have been proven to have microbicidal properties through the excess production of reactive oxygen species and damaging the microbial membrane, making them favorable to be used as an efficient antimicrobial agent [14,15].

Recent reports indicate that zinc oxide nanoparticles (ZnO NPs) are considered as a next-generation nano-antimicrobial agent against human pathogenic multi-drug-resistant bacteria and fungi [16]. Much more focus and work are required urgently for the novel approaches to identify effective new antimicrobial agents, both selective and broad spectrum, to sustainably combat antimicrobial resistance [17,18]. ZnO NPs have been studied and utilized in several biomedical applications, such as anti-aging, bio-imaging, drug delivery, and antimicrobial agent, to treat various skin infections [19–21]. According to previous research, ZnO NPs have significant antifungal activities against *Botrytis cinerea* and *Penicillium expansum*, and the inhibitory effects increased as ZnO NPs concentrations increased [22]. These nanoparticles also have a large surface area to volume proportion and show unique physicochemical properties, such as porosity, crystallinity, particle size, and morphology, which are highly accounted for the biomedical applications. In addition, the scientific toxicity studies indicate that the ZnO NP is a preferable option as an antimicrobial agent because it has low toxicity and is compatible with humans while toxic to microorganisms [23].

Fungal infections have emerged as a significant health issue associated to an increasing number of people who have immune system deficiencies. *Saccharomyces cerevisiae* is a unicellular fungus, which is related with infections ranging from vaginitis in healthy patients and cutaneous infections, to systemic bloodstream infections and infections of essential organs, such as lungs, esophagus, peritoneum, urinary tract, etc., in immunocompromised and critically ill patients. However, much less effort has been made to investigate the response of *S. cerevisiae* to antifungal treatment. Remarkably, the genetic tractability of *S. cerevisiae* has made it a model organism for the study of fundamental issues in fungal biology [24,25]. Hence, in this work, we investigated the effect of ZnO NPs on the growth and surface morphology of *S. cerevisiae*. The findings of the study might be helpful to incorporate and utilize ZnO NPs as an antifungal agent in treating the infections caused by *S. cerevisiae*.

2. Materials and Methods

2.1. Characterization of ZnO NPs

Chemically synthesized ZnO nanopowder (particle size < 100 nm) was acquired from Sigma-Aldrich. The surface morphology and average particle size were identified using Scanning Electron Microscope with Energy Dispersive X-ray (SEM-EDX) (JSM-6701F, JOEL, Tokyo, Japan) with a working distance of 4.7 mm and an acceleration voltage of 4 kV. The elemental composition of the ZnO nanopowder was confirmed by EDX spectrum. The X-ray diffractometer (XRD) (Lab X, SHIMADZU, XRD-6000, Tokyo, Japan), operated at an

Coatings **2022**, 12, 1988 3 of 12

angle of 20 with 40 V and 30 mA current, was applied to confirm the crystalline nature and crystalline size of the nanomaterial. Further, Fourier transform infrared (FTIR) spectroscopy (Perkin-Elmer Spectrum RX1, Waltham, MA, USA) was performed to confirm the chemical composition of ZnO NPs.

2.2. Preparation of ZnO NPs Suspension

The stock solution of ZnO NPs (300 $\mu g/mL$) was prepared in Sabouraud Dextrose Broth (SDB) and ultra-sonicated for 30 min at 37 kHz to obtain an even and homogenous solution. The stock was later diluted with SDB to get the various working concentrations.

2.3. Exposure of Yeast to ZnO NPs

The stock culture of *S. cerevisiae* (ATCC 9763) was obtained from the Faculty of Science, Universiti Tunku Abdul Rahman, and then sub cultured to the mid-log phase in SDB broth. The yeast suspension with OD of 0.1 at 600 nm during its mid-log phase at 5 h of sub-culture was exposed to different concentrations of ZnO NPs (5, 10, 25, 50, 100, and 150 μ g/mL) and incubated for 24 h at room temperature. The yeast culture added with amphotericin B (50 μ g/mL) acted as the positive control, while the yeast culture without ZnO NPs was the negative control.

2.4. Growth Inhibition Test

The turbidity method was used to ascertain the fungi-static reaction of ZnO NPs. The turbidity of yeast suspensions exposed with the six concentrations of ZnO NPs and the two controls were measured after incubation at room temperature ($25\,^{\circ}$ C) for 24 h using a visibleectrophotometer (Libra S4, Dichromium, Biochrom, Cambridge, UK) at 600 nm. The optical density of each concentration of ZnO NPs suspension was deducted from the test reading to exclude interference from NPs. Meanwhile, SDB was taken as blank for each measurement. The final absorbance values were taken to analyze the impact of the six concentrations of ZnO NPs on the growth of the yeast. The percentage of inhibition of *S. cerevisiae* after ZnO NPs treatment was calculated by using Equation (1).

Percentage of growth inhibition =
$$\frac{\text{OD negative control} - \text{OD test}}{\text{OD negative control}} \times 100\%$$
 (1)

* OD = the optical density at 600 nm.

2.5. Fourier Transform Infrared (FTIR) Spectroscopy

FTIR analysis was done to observe the involvement of surface functional groups of the yeast cell wall in facilitating the binding of ZnO NPs on the cell surface. A volume of 3 mL yeast cell suspension from treatment with 150 μ g/mL of ZnO NPs was taken and centrifuged for 10 min at $6000 \times g$ after incubation for 24 h. The pellet was washed with 1× PBS. The process was repeated three times, and the pellet was freeze-dried to eliminate moisture. Then the pellet was subjected to FTIR analysis (Perkin-Elmer, Spectrum RX1, Waltham, MA, USA) at the range of 4000 to 400 cm⁻¹ [21].

2.6. SEM-EDX Analysis

The harvested yeast cells pellet was washed with $1 \times PBS$ for 3 times by centrifuging at $6000 \times g$ for 10 min. The cells were then fixed with 2.5% glutaraldehyde in PBS overnight. The samples were washed with $1 \times PBS$ three times and then with distilled water. Further, the dehydration was done with increasing concentrations of ethanol, at 50%, 75%, and 95%, and the final step of the dehydration process was repeated three times with 100% absolute alcohol, followed by critical point drying and sputter coating. The pre-treated cells were then examined with scanning electron microscopy (JEOL JSM 6710F, Tokyo, Japan) [21].

Coatings **2022**, 12, 1988 4 of 12

2.7. Statistical Analysis

All the tests were conducted in triplicates, and the data are presented as mean \pm standard deviation. The data were processed by using one-way analysis of variance (ANOVA, IBMM SPSS) to analyze the variance triggered by ZnO NPs towards the yeast.

3. Results and Discussion

3.1. Characterization of ZnO NPs

The SEM analysis was used to view the surface morphology and average particle size of ZnO NPs. The SEM image showed sphere-shaped NPs with rods, as shown in Figure 1A. The average size of the particles was measured to be 49.85 nm, with a range of 31.4 to 66.3 nm. The EDX analysis verified the element composition of ZnO NPs. Based on the peaks shown in Figure 1B, the zinc and oxygen molecules were confirmed to be present in the ZnO nanopowder studied.

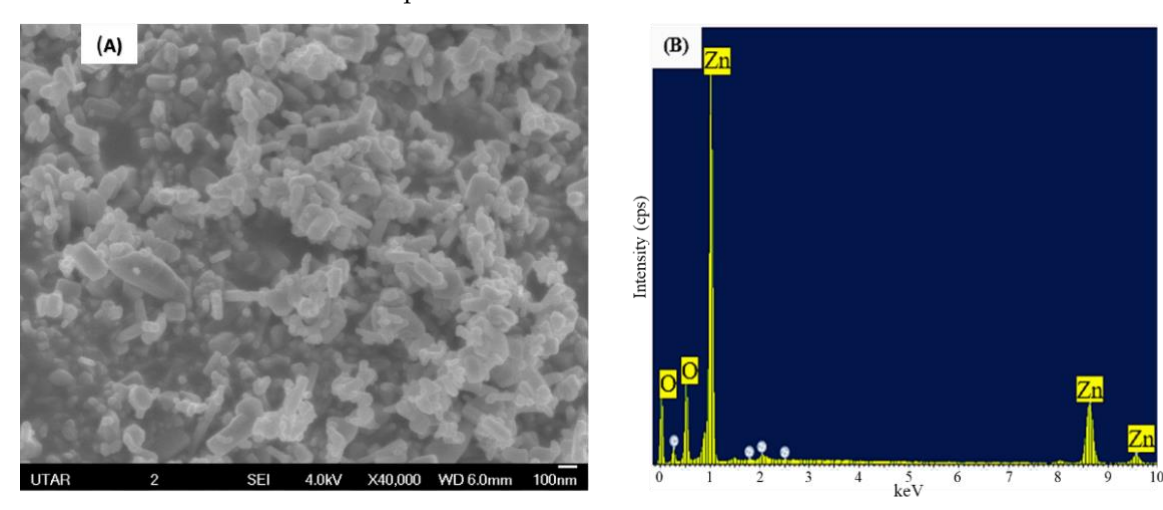


Figure 1. Surface morphology and elemental composition of ZnO NPs; SEM (**A**) and EDX spectrum (**B**).

The XRD spectrum shown in Figure 2 revealed that the ZnO NPs are in a hexagonal wurtzite crystalline structure according to ICDD-PDF-4-2018-01-070-8070 [26]. The average crystalline size of ZnO NPs was calculated to be 37.29 nm by Debye Scherrer's formula. Further, the FTIR spectrum displayed in Figure 3 illustrates the peaks at 3425, 1628, and 524 cm $^{-1}$. The peak near 3400 and 3600 cm $^{-1}$ is ascribed to O-H vibration on the surface of ZnO nanoparticles, the peak near 1634 cm $^{-1}$ corresponds to Zn-O stretching, and the peak at 400–800 cm $^{-1}$ represents stretching of ZnO nanoparticles [27,28].

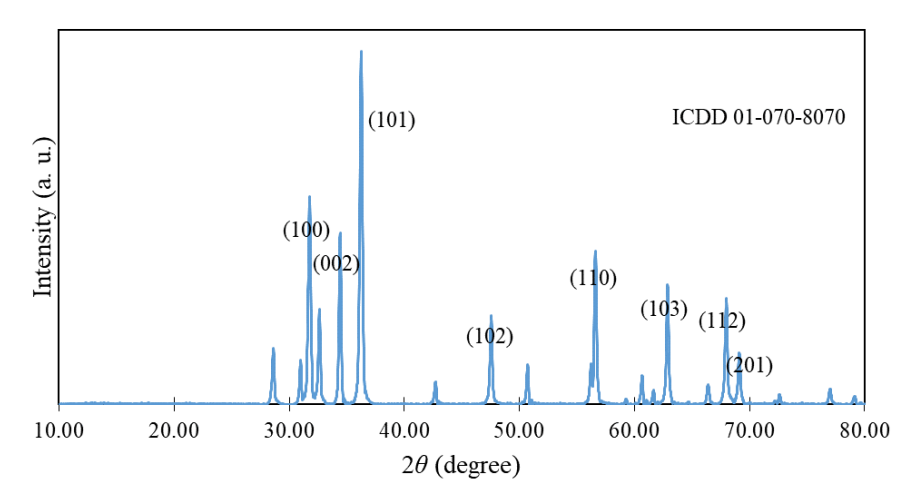


Figure 2. XRD analysis of ZnO NPs.

Coatings 2022, 12, 1988 5 of 12

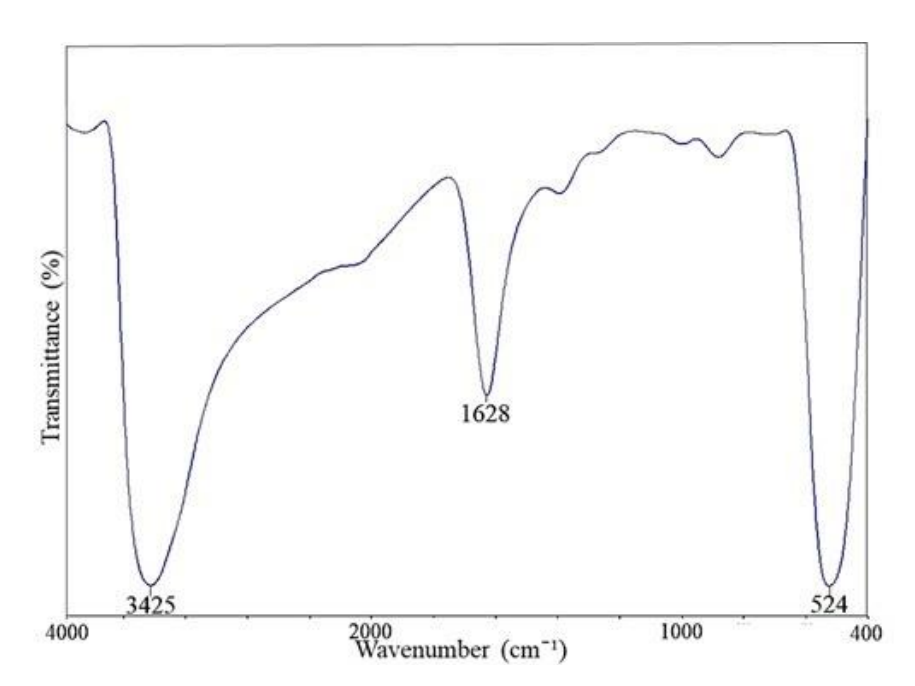


Figure 3. FTIR Spectrum of ZnO NPs.

3.2. Growth Inhibition Test

The exposure of yeast cells to the different concentrations of ZnO NPs was performed to report the antifungal effect of ZnO NPs on *S. cerevisiae*. The present study results showed that the treatment of ZnO NPs on *S. cerevisiae* resulted in a significant (p < 0.05) growth reduction at 24 h with the reported values of 7.04 ± 0.64 , 18.85 ± 1.92 , 33.38 ± 1.35 , 40.38 ± 1.81 , 61.13 ± 4.89 , and $70.30 \pm 3.19\%$ for 5, 10, 25, 50, 100, and $150 \,\mu\text{g/mL}$ ZnO NPs, respectively (Figure 4). A growth reduction of $88.65 \pm 1.49\%$ was reported in positive control treated with amphotericin B ($50 \,\mu\text{g/mL}$).

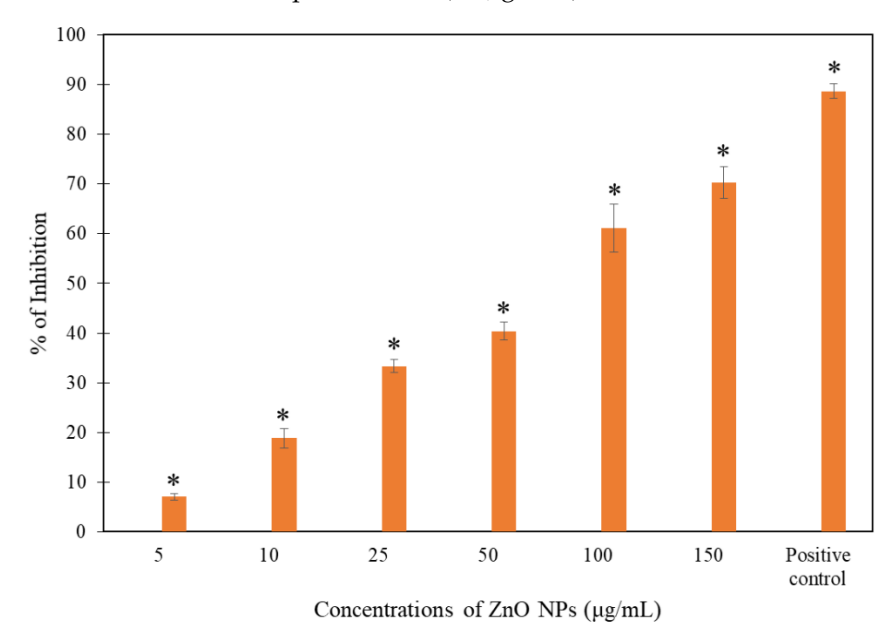


Figure 4. The percentage of growth inhibition on *S. cerevisiae* after treatment with six distinct concentrations of ZnO NPs for 24 h at 25 °C in SDB. The values plotted in the graph are in mean \pm standard deviation. * Demonstrates the significant difference between control and yeast suspension treated with ZnO NPs at p < 0.05.

The gradual decrease in the growth of yeast cells was observed as the concentration of nanoparticles increased, as shown in Figure 4, indicating a dose-dependent growth

Coatings 2022, 12, 1988 6 of 12

inhibition of *S. cerevisiae*. A study from Nasrollahi et al. [29], which studied the antifungal activity of silver nanoparticles (Ag NPs) on *Candida albicans* and *S. cerevisiae*, reported 50% fungal inhibition when treated with 0.5 and 4 mg/mL of Ag NPs, respectively, at 35 °C for 24 h. Moreover, Khan et al. [30] reported that the maximum zone of inhibition of *C. albicans* when exposed to 0.5 mg/mL of ZnO NPs for 48 h at 37 °C was 20 mm through the disc-diffusion method. The minimum inhibitory concentration (MIC) and minimum fungicidal concentration (MFC) of ZnO NPs on *C. albicans* at 35 °C for 48 h were 128 and 256 μ g/mL respectively [31]. The MIC of ZnO NPs against *Alternaria alternata*, *Aspergiluus niger*, *Botrytis cinerea*, *Fusarium oxysporum*, and *Peniciilium expansum* at 28 °C for 72 h was 64, 16, 128, 64, and 128 μ g/mL, respectively [32]. Likewise, in this present study, the ZnO NPs showed dose-dependent growth inhibition of *S. cerevisiae*, as the concentration of ZnO NPs increased from 5 to 150 μ g/mL, the growth of inhibition rate also increased from 7.04 \pm 0.64 to 70.30 \pm 3.19%.

3.3. Surface Interaction of ZnO NPs on the Yeast Cell Wall

FTIR analysis was used to inspect the related functional groups involved in the interaction of ZnO NPs onto the surface of *S. cerevisiae*, as shown in Table 1. The FTIR spectrum of ZnO NPs treated *S. cerevisiae* (Figure 5) illustrated the likely involvement of hydroxyl group (3422 cm⁻¹), alkene (2928, 2374, and 2345 cm⁻¹), amide I (1648 cm⁻¹), carbonyl, and alkene (1402 cm⁻¹) and phosphate groups (1051 cm⁻¹) of the yeast cell wall in the binding of ZnO NPs to yeast surface, respectively.

Table 1. Possible involvement of functional groups in the surface binding of ZnO NPs on the year	east
cell surface.	

Absorption (cm ⁻¹)	Molecular Motion	Functional Group	Biomolecules
$3435 \rightarrow 3422$	O-H with N-H stretching modes	Alcohol, secondary amide	Proteins, Polysaccharides, Chitin
2928	C-H groups	Ergosterol	Lipids
2374, 2345	CH ₂ vibration	Alkene group	Hydrocarbon
$1639 \rightarrow 1648$	C=O stretching, N-H bending	Amide I	Polypeptides
$1398 \rightarrow 1402$	C=O of COO ⁻ symmetric stretching vibrations in proteins, CH ₂ wagging vibrations in lipids, and β (1–3) glucans	Carbonyl group, Alkene group	Lipids, Proteins, Polysaccharides
$1081 \rightarrow 1051$	C-O mainly by vibrations and absorptions of polysaccharides and phosphate groups	Polysaccharides, phosphate group	Polysaccharides, mainly glucans and mannans & Phospholipids

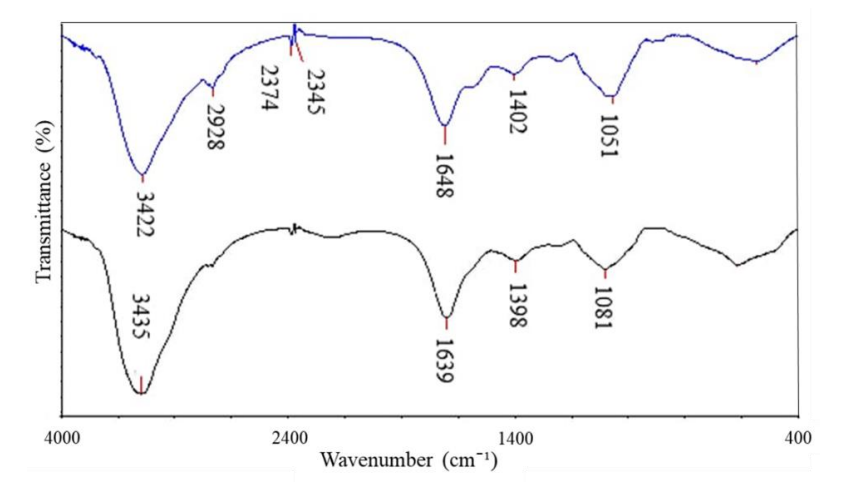


Figure 5. FTIR spectrum of *S. cerevisiae* treated with 150 μ g/mL ZnO NPs. Black line denotes the negative control, while blue line denotes the sample treated with 150 μ g/mL ZnO NPs.

Coatings **2022**, 12, 1988 7 of 12

The area between 3435 and 3422 cm⁻¹ was mainly assigned to O-H and N-H groups stretching of proteins, polysaccharides, particularly chitin [33,34]. According to studies from Kiwi and Nadtochenko [35] and Fang et al. [36], the permeability of the lipids on the cell wall could be affected when the nanoparticles attached to the –CH groups on the cell membrane, which will be shown in the peak range from 3100 to 2800 cm⁻¹. This peak region is also important to indicate the adverse effect of the nanoparticles on the cell wall [37,38]. Hence, the newly formed peaks in the ZnO NPs treated samples at 2928 cm⁻¹ may possibly be associated with the involvement of C-H groups of lipids in binding of NPs, the lipid might be ergosterol. There were also other two peaks, 2374 and 2345 cm⁻¹ resulting from the asymmetric C-H stretching of hydrocarbon [39].

According to studies by Burgula et al. [40] and Eckhardt et al. [41], when the ions are discharged from the nanoparticles, they will start to target the organic compounds such as amino acids, and this will lead to an alteration in the conformation of the protein. This alteration happened when the peak shifted from 1639 to 1648 cm $^{-1}$, which resulted from the stretching vibration of C=O groups by intramolecular native β -pleated sheet structures [42]. The increase in absorptions of β -pleated was possibly due to the denaturation of the secondary structure to its primary conformation [34]. Naumann [33] suggested that the region of protein amide I bands frequently overlaps with nucleic acid, and any changes in hydrogen bonds in the secondary structure will affect the vibration in amide I region, which is important to determine the secondary conformation of protein [43]. The peaks observed in the region 1398 and 1402 cm $^{-1}$ were contributed by C=O stretching uniformly of COO in polypeptides [44]. On top of that, the peak number shown within this region may be dominated by the alkene vibration of the trimethylamine group in phosphatidylcholine [45]. Besides, Casal and Mantsch [46] reported that the wagging vibrations in lipids and β (1–3) glucans would lead to the shifting of peak within this region.

The peaks at 1081 and 1051 cm⁻¹ are typically corresponded to polysaccharides, specifically glucans and mannans, which are mostly found on the cell wall of the yeast [47]. This was possibly due to the absorption of carbohydrates and insignificant contribution from phosphate groups in phospholipids covered in the spectral area between 1200 cm⁻¹ and 900 cm⁻¹ [47]. In addition, Jiang et al. [48] reported that when bacteria are treated with metal oxide nanoparticles, the C-O bond in carbohydrates will be weakened due to the increment in the absorption energy as a result of the bonding formation between hydrogen with oxides and the subsequent radicals generated during the oxidation will change the configuration of polysaccharides [41], which, in turn, may compromise the membrane integrity and lead to cell death. Overall, the FTIR spectrum of *S. cerevisiae* treated with ZnO NPs demonstrated the possible involvement of different functional groups, such as hydroxyl, amides, alkene, and phosphate from phospholipids, polypeptides, polysaccharides, and ergosterol, in binding of ZnO NPs on the cell surface which might have brought the loss of membrane integrity and death of yeast cells.

3.4. Scanning Electron Microscopy

The SEM was used to visualize the morphological changes in *S. cerevisiae* after exposure to ZnO NPs for 24 h. In the yeast suspensions without any treatment, as shown in Figure 6A, the yeast cells appeared in ovoid shape with slight elongation and intact cell membrane. The treatment of ZnO NPs on yeast cells caused several morphological alterations on the cell surface. Based on Figure 6B, the yeast cell treated with $100~\mu g/mL$ of ZnO NPs after 24 h showed rupture of the cell membrane. Besides, there were several invaginations and pitting observed on the cell surface (Figure 6C). Similar results were found in a study by Kieliszek et al. [49] where *C. albicans* showed shrinkage and fragmented vacuoles in the cells when they were exposed to 20~mg/L of selenium nanoparticles at 24 h.

Coatings **2022**, 12, 1988 8 of 12

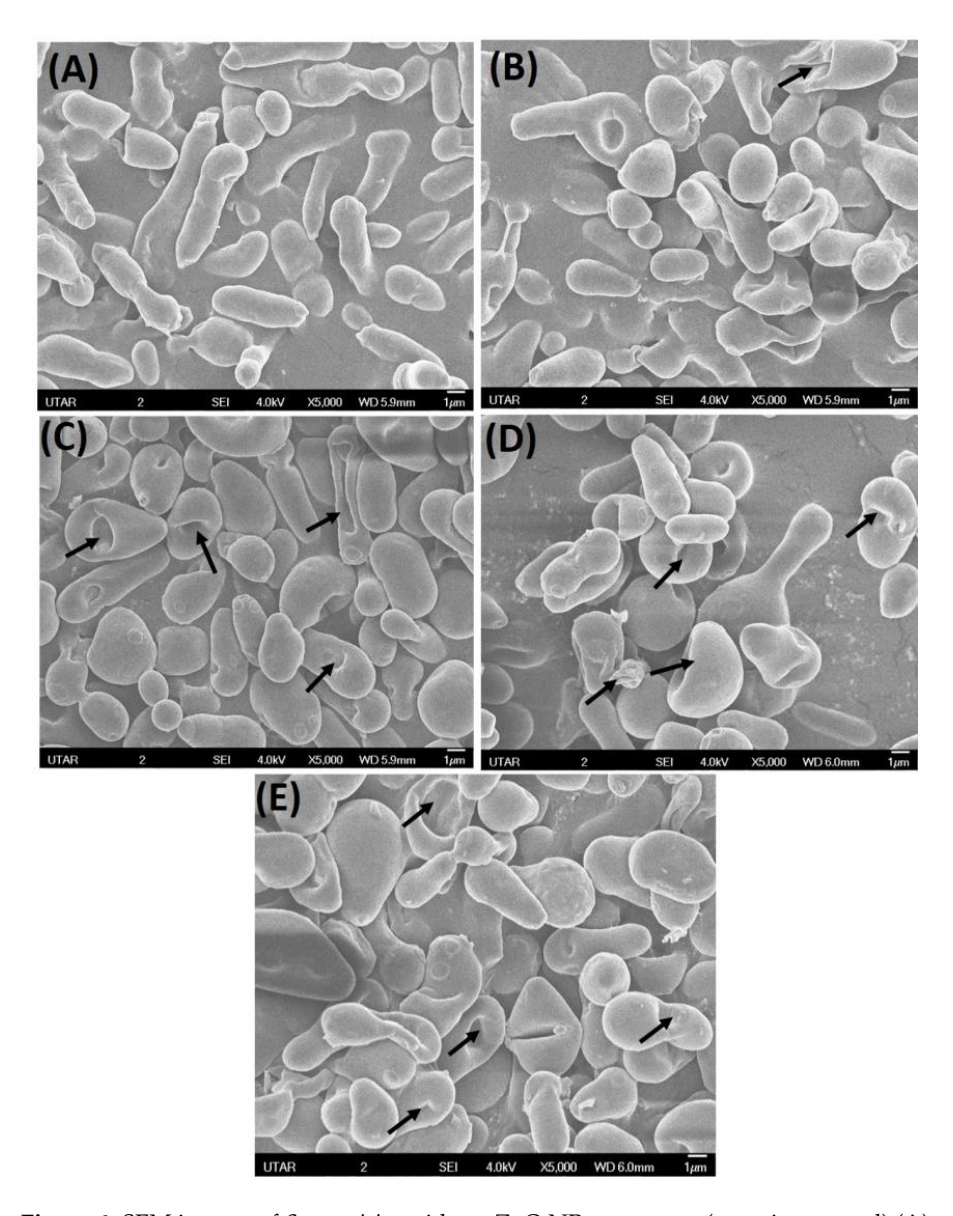


Figure 6. SEM images of *S. cerevisiae* without ZnO NPs treatment (negative control) (**A**), treated with $100~\mu g/$ mL of ZnO NPs showing rupture of cell membrane (**B**) and regional invagination and pitting of yeast cell surface (**C**), treated with $150~\mu g/$ mL of ZnO NPs showing cell wrinkle (**D**), and cracks and deformity on the cells (**E**) at 24 h.

In the present study, when the concentration of ZnO NPs increased to 150 μ g/mL of ZnO NPs, the yeast cell showed wrinkles, as seen in Figure 6D, and deformity on the cells, as shown in Figure 6E at 24 h. Similarly, *S. cerevisiae* was reported to show wrinkles when it was subjected to environmental stress [50]. Further, a study by Radhakrishnan et al. [51] evidenced that the *C. albicans* treated with 40 μ g/mL of Ag NPs demonstrated wrinkle, bumpy and irregular external cell membrane, and these were believed to be responsible for the destruction of the external cell structure and plasma membrane. Besides, our earlier studies on bacteria *S. pyogenes* and *P. aeruginosa* reported similar morphological damages when treated with ZnO NPs at 24 h, as demonstrated in the present study [52,53]. For the cytotoxicity effects of ZnO NPs on fungi, researchers have proposed several possible mechanisms, as shown in Figure 7. These mechanisms included the accumulation of ROS on the surface of fungi [54,55], release of Zn²⁺ ions [56,57], interaction and accumulation of ZnO NPs on the cell surface of fungi [58], distortion and interference of physiological processes

Coatings 2022, 12, 1988 9 of 12

which render the normal function of the cell membrane [57,59] and the morphological changes of the cell, which can lead to cell death [59,60].

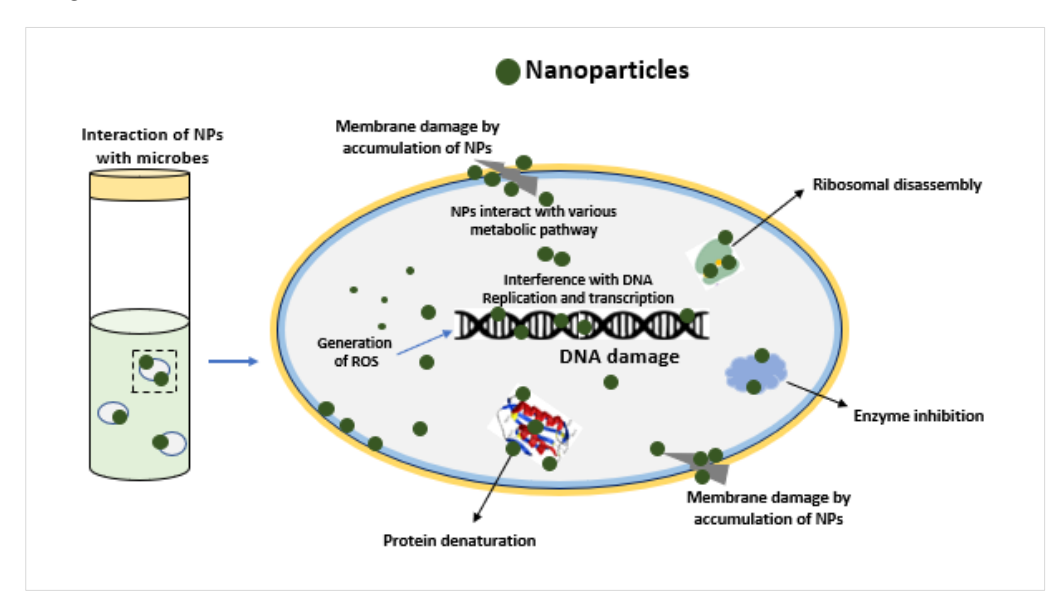


Figure 7. The possible antifungal mechanisms of NPs, including the generation of ROS, rupture of the cell membrane, DNA damage, and enzyme inhibition.

4. Conclusions

The present study demonstrated the dose-dependent growth inhibitory activity of ZnO NPs on $\it S. cerevisiae.$ The treatment ZnO NPs caused significant growth inhibition of $\it S. cerevisiae.$ from 5 µg/mL of ZnO NPs at 24 h. In addition, the treatment of ZnO NPs resulted in the deformity and rupture of cell membrane, which could have possibly led to cell death. Further, the hydroxyl group, alkene, amides, carbonyl, and phosphate groups from the phospholipids, polysaccharides, polypeptides, and ergosterol of the yeast cell wall were identified to be responsible for binding of ZnO NPs on the cell surface. The present investigation might be helpful to explore the application of ZnO NPs as an effective antifungal agent in treating infections caused by $\it S. cerevisiae.$

Author Contributions: Conceptualization, S.D., L.S.W., A.C.T.A. and M.A.; Methodology, S.D., L.S.W., A.C.T.A. and M.A.; Investigation, E.P.T. and S.D.; Resources, S.D. and L.S.W.; Visualization, A.K.J.; Writing—original draft preparation, E.P.T., S.D., R.R. and L.S.W.; Writing—review and editing, S.K.S., M.A., V.S., M.S. and S.S. All authors have read and agreed to the published version of the manuscript.

Funding: This research work was funded by Universiti Tunku Abdul Rahman Research Fund (IPSR/RMC/UTARRF/2020-C2/S06) and Ministry of Education, Malaysia (Grant No. FRGS-1-2014-SG03-INTI-02-1).

Institutional Review Board Statement: Not applicable.

Informed Consent Statement: Not applicable.

Data Availability Statement: The data used to support the findings of this study will be provided on request.

Conflicts of Interest: The authors declare that there is no conflict of interest regarding the publication of this paper.

Coatings 2022, 12, 1988 10 of 12

References

 Zhang, H.; Zhu, A. Emerging invasive fungal infections: Clinical features and controversies in diagnosis and treatment processes. *Infect. Drug Resist.* 2020, 13, 607–615. [CrossRef] [PubMed]

- 2. Chang, Y.-L.; Yu, S.-J.; Heitman, J.; Wellington, M.; Chen, Y.-L. New facets of antifungal therapy. *Virulence* **2016**, *8*, 222–236. [CrossRef] [PubMed]
- 3. Souza, A.C.; Amaral, A.C. Antifungal Therapy for Systemic Mycosis and the Nanobiotechnology Era: Improving Efficacy, Biodistribution and Toxicity. *Front. Microbiol.* **2017**, *8*, 336. [CrossRef]
- 4. Sousa, F.; Ferreira, D.; Reis, S.; Costa, P. Current insights on antifungal therapy: Novel nanotechnology approaches for drug delivery systems and new drugs from natural sources. *Pharmaceuticals* **2020**, *13*, 248. [CrossRef] [PubMed]
- 5. Djearamane, S.; Wong, L.S.; Lim, Y.M.; Lee, P.F. Oxidative stress effects of zinc oxide nanoparticles on fresh water microalga *Haematococcus pluvialis*. *Ecol. Environ. Conserv.* **2020**, *26*, 2020–2663.
- 6. Zhang, Z.; Wang, H.; Chen, Z.; Wang, X.; Choo, J.; Chen, L. Plasmonic colorimetric sensors based on etching and growth of noble metal nanoparticles: Strategies and applications. *Biosens Bioelectron.* **2018**, *114*, 52–65. [CrossRef]
- 7. Soto-Robles, C.A.; Luque, P.A.; Gómez-Gutiérrez, C.M.; Nava, O. Vilchis-Nestor, A.R.; Lugo-Medina, E. Ranjithkumar. R. Castro-Beltrán, A. Study on the effect of the concentration of *Hibiscus sabdariffa* extract on the green synthesis of ZnO nanoparticles. *Results Phys.* **2019**, *15*, 1–8. [CrossRef]
- Djearamane, S.; Wong, L.S.; Lim, Y.M.; Lee, P.F. Cytotoxic Effects of Zinc Oxide Nanoparticles on Chlorella vulgaris. Pollut. Res. 2019, 38, 479–484.
- 9. Ranjithkumar, R.; Selvam, K.; Shanmugavadivu, M. Antimicrobial coated textile via biogenic synthesis silver nanoparticles. J. Green Sci. Technol. 2013, 1, 111–113.
- Rauf, M.A.; Oves, M.; Rehman, F.U.; Khan, A.R.; Husain, N. Bougainvillea flower extract mediated zinc oxide's nanomaterials for antimicrobial and anticancer activity. *Biomed. Pharmacother.* 2019, 116, 108983. [CrossRef] [PubMed]
- 11. Jilani, A.; Othman, M.H.D.; Ansari, M.O.; Oves, M.; Hussain, S.Z.; Khan, I.U.; Abdel-wahab, M.S. Structural and optical characteristics, and bacterial decolonization studies on non-reactive RF sputtered Cu–ZnO@ graphene-based nanoparticles thin films. *J. Mater. Sci.* **2019**, *54*, 6515–6529. [CrossRef]
- 12. Djearamane, S.; Ravintharan, T.; Liang, S.X.T.; Wong, L.S. Sensitivity of *Proteus vulgaris* to Zinc Oxide Nanoparticles. *Sains Malays*. **2022**, *51*, 1353–1362. [CrossRef]
- 13. Bharathi, D.; Ranjithkumar, R.; Chandar Shekar, B.; Bhuvaneshwari, V. Preparation of chitosan coated zinc oxide nanocomposites for enhanced antibacterial and photocatalytic activity: As a bionanocomposite. *Int. J. Biol. Macromol.* **2019**, 129, 989–996. [CrossRef] [PubMed]
- 14. Jin, S.-E.; Jin, H.-E. Antimicrobial Activity of Zinc Oxide Nano/Microparticles and Their Combinations against Pathogenic Microorganisms for Biomedical Applications: From Physicochemical Characteristics to Pharmacological Aspects. *Nanomaterials* **2021**, *11*, 263. [CrossRef] [PubMed]
- 15. Munir, M.U.; Ahmed, A.; Usman, M.; Salman, S. Recent advances in nanotechnology-aided materials in combating microbial resistance and functioning as antibiotics substitutes. *Int. J. Nanomed.* **2020**, *15*, 7329. [CrossRef]
- 16. Dizaj, S.M.; Lotfipour, F.; Barzegar-Jalali, M.; Zarrintan, M.H.; Adibkia, K. Antimicrobial activity of the metals and metal oxide nanoparticles. *Mater. Sci. Eng. C* **2014**, *44*, 278–284. [CrossRef]
- 17. Theuretzbacher, U.; Outterson, K.; Engel, A.; Karlén, A. The global preclinical antibacterial pipeline. *Nat. Rev. Genet.* **2019**, *18*, 275–285. [CrossRef]
- 18. Li, W.; Separovic, F.; O'Brien-Simpson, N.M.; Wade, J.D. Chemically modified and conjugated antimicrobial peptides against superbugs. *Chem. Soc. Rev.* **2021**, *50*, 4932–4973. [CrossRef]
- 19. Djearamane, S.; Lim, Y.M.; Wong, L.S.; Lee, P.F. Cellular accumulation and cytotoxic effects of zinc oxide nanoparticles in microalga *Haematococcus pluvialis*. *PeerJ* **2019**, 7, e7582. [CrossRef]
- 20. Maheswaran, H.; Wong, L.S.; Dhanapal, A.C.T.A.; Narendhirakannan, R.T.; Janakiraman, A.K.; Djearamane, S. Toxicity of zinc oxide nanoparticles on human skin dermal cells. *J. Exp. Biol. Agric. Sci.* **2021**, *9*, S95–S100. [CrossRef]
- 21. Djearamane, S.; Loh, Z.C.; Lee, J.J.; Wong, L.S.; Rajamani, R.; Luque, P.A.; Gupta, P.K.; Liang, S.X.T. Remedial Aspect of Zinc Oxide Nanoparticles Against Serratia marcescens and Enterococcus faecalis. Front. Pharmacol. 2022, 13, 1–13. [CrossRef] [PubMed]
- 22. He, L.; Liu, Y.; Mustapha, A.; Lin, M. Antifungal activity of zinc oxide nanoparticles against *Botrytis cinerea* and *Penicillium expansum*. *Microbiol*. *Res.* **2011**, *166*, 207–215. [CrossRef] [PubMed]
- 23. Sirelkhatim, A.; Mahmud, S.; Seeni, A.; Kaus, N.H.M.; Ann, L.C.; Bakhori, S.K.M.; Mohamad, D. Review on Zinc Oxide Nanoparticles: Antibacterial Activity and Toxicity Mechanism. *Nano-Micro Lett.* **2015**, *7*, 219–242. [CrossRef] [PubMed]
- 24. Munoz, P.; Bouza, E.; Cuenca-Estrella, M.; Eiros, J.M.; Pérez, M.J.; Sánchez-Somolinos, M.; Peláez, T. *Saccharomyces cerevisiae* Fungemia: An Emerging Infectious Disease Source: Clinical Infectious Diseases. *Oxf. J.* **2005**, *40*, 1625–1634.
- 25. Bojsen, R.; Regenberg, B.; Folkesson, A. Saccharomyces cerevisiae biofilm tolerance towards systemic antifungals depends on growth phase. *BMC Microbiol.* **2014**, *14*, 1–10. [CrossRef]
- 26. Michlik, T.; Schmid, M.; Rosin, A.; Gerdes, T.; Moos, R. Mechanical coating of zinc particles with Bi₂O₃-Li₂O-ZnO glasses as anode material for rechargeable zinc-based batteries. *Batteries* **2018**, *4*, 12. [CrossRef]
- 27. Ahmad, W.; Kalra, D. Green synthesis, characterization and anti-microbial activities of ZnO nanoparticles using *Euphorbia hirta* leaf extract. *J. King Saud Univ.-Sci.* **2020**, *32*, 2358–2364. [CrossRef]

Coatings **2022**, 12, 1988 11 of 12

28. Saini, M.; Yadav, S.; Rani, N.; Mushtaq, A.; Rawat, S.; Saini, K. Antibacterial study of nanosized zinc oxide (F1) against various gram-positive and gram-negative bacteria. *Mater. Today Proc.* **2022**, *67*, 852–857. [CrossRef]

- 29. Nasrollahi, A.; Pourshamsian, K.H.; Mansourkiaee, P. Antifungal activity of silver nanoparticles on some of fungi. *Int. J. Nano Dim.* **2011**, *1*, 233–239.
- 30. Khan, M.F.; Ansari, A.H.; Hameedullah, M.; Ahmad, E.; Husain, F.M.; Zia, Q.; Aliev, G. Flower-shaped ZnO nanoparticles synthesized by a novel approach at near-room temperatures with antibacterial and antifungal properties. *Int. J. Nanomed.* **2014**, 9, 853–864. [CrossRef]
- 31. Miri, A.; Mahdinejad, N.; Ebrahimy, O.; Khatami, M.; Sarani, M. Zinc oxide nanoparticles: Biosynthesis, characterization, antifungal and cytotoxic activity. *Mater. Sci. Eng. C* **2019**, *104*, 109981. [CrossRef] [PubMed]
- 32. Jamdagni, P.; Khatri, P.; Rana, J.S. Green synthesis of zinc oxide nanoparticles using flower extract of *Nyctanthes arbor-tristis* and their antifungal activity. *J. King Saud Univ.—Sci.* **2018**, *30*, 168–175. [CrossRef]
- 33. Naumann, D. FT-Infrared and FT-Raman spectroscopy in biomedical research. Appl. Spectrosc. Rev. 2001, 36, 239–298. [CrossRef]
- 34. Burattini, E.; Cavagna, M.; Dell'Anna, R.; Campeggi, F.M.; Monti, F.; Rossi, F.; Torriani, S. A FTIR microspectroscopy study of autolysis in cells of the wine yeast *Saccharomyces cerevisiae*. *Vib. Spectrosc.* **2008**, *47*, 139–147. [CrossRef]
- 35. Kiwi, J.; Nadtochenko, V. Evidence for the mechanism of photocatalytic degradation of the bacterial wall membrane at the TiO₂ interface by ATR–FTIR and laser kinetic spectroscopy. *Langmuir* **2005**, *21*, 4631–4641. [CrossRef]
- 36. Fang, J.; Lyon, D.Y.; Wiesner, M.R.; Dong, J.; Alvarez, P.J. Effect of a fullerene water suspension on bacterial phospholipids and membrane phase behaviour. *Environ. Sci. Technol.* **2007**, *41*, 2636–2642. [CrossRef] [PubMed]
- 37. Sivakesava, S.; Irudayaraj, J.; Debroy, C. Differentiation of microorganisms by FTIR-AIR and NIR spectroscopy. *Trans. ASAE* **2004**, 47, 951–957. [CrossRef]
- 38. Mura, S.; Greppi, G.; Marongiu, M.L.; Roggero, P.P.; Ravindranath, S.P.; Mauer, L.J.; Irudayaraj, J. FTIR nanobiosensors for *Escherichia coli* detection. *Beilstein J. Nanotechnol.* **2012**, *3*, 485–492. [CrossRef] [PubMed]
- 39. Sivakumar, P.; Nethradevi, C.; Renganathan, S. Synthesis of silver nanoparticles using *Lantana Camara* fruit extract and its effect on pathogens. *Asian J. Pharm. Clin. Res.* **2012**, *5*, 97–101.
- Burgula, Y.; Khali, D.; Kim, S.; Krishnan, S.S.; Cousin, M.A.; Gore, J.P.; Mauer, L.J. Detection of Escherichia coli O157:H7 and Salmonella typhimurium using filtration followed by Fourier-transform infrared spectroscopy. J. Food Prot. 2006, 69, 1777–1784.
 [CrossRef] [PubMed]
- 41. Eckhardt, S.; Brunetto, P.S.; Gagnon, J.; Priebe, M.; Giese, B.; Fromm, K.M. Nanobio Silver: Its Interactions with Peptides and Bacteria, and Its Uses in Medicine. *Chem. Rev.* **2013**, *113*, 4708–4754. [CrossRef] [PubMed]
- 42. Correa-Garcia, S.; Bermudez-Moretti, M.; Travo, A.; Dekeris, G.; Fortar, I. FTIR spectroscopic metabolome analysis of lyophilized and fresh *Saccharomyces cerevisiae* cells. *Anal. Methods* **2014**, *6*, 1855–1861. [CrossRef]
- 43. Gorgulu, S.T.; Dogan, M.; Severcan, F. The characterization and differentiation of higher plants by Fourier transform infrared spectroscopy. *Appl. Spectrosc.* **2007**, *61*, 300–308. [CrossRef] [PubMed]
- 44. Lasch, P.; Boese, M.; Pacifico, A.; Diem, M. FT-IR spectroscopic investigations of single cells on the subcellular level. *Vib. Spectrosc.* **2002**, *28*, 147–157. [CrossRef]
- 45. Cieślik-Boczula, K.; Czarnik-Matusewicz, B.; Perevozkina, M.; Rospenk, M. MCR-ALS as an effective tool for monitoring subsequent phase transitions in pure and doped DPPC liposomes. *R. Soc. Chem. Adv.* **2015**, *5*, 40455–40464. [CrossRef]
- 46. Casal, H.L.; Mantsch, H.H. Polymorphic phase behaviour of phospholipid membranes studied by infrared spectroscopy. *Biochim. Biophys. Acta* **1984**, 779, 381–401. [CrossRef] [PubMed]
- 47. Plata, M.R.; Koch, C.; Wechselberger, P.; Herwig, C.; Lendl, B. Determination of carbohydrates present in *Saccharomyces cerevisiae* using mid-infrared spectroscopy and partial least squares regression. *Anal. Bioanal. Chem.* **2013**, 405, 8241–8250. [CrossRef] [PubMed]
- 48. Jiang, W.; Yang, K.; Vachet, R.W.; Xing, B. Interaction between oxide nanoparticles and biomolecules of the bacterial cell envelope as examined by infrared spectroscopy. *Langmuir* **2010**, *26*, 18071–18077. [CrossRef] [PubMed]
- 49. Kieliszek, M.; Błażejak, S.; Bzducha-Wróbel, A.; Kurcz, A. Effects of Selenium on Morphological Changes in *Candida utilis* ATCC 9950 Yeast Cells. *Biol. Trace Elem. Res.* **2015**, *169*, 387–393. [CrossRef]
- 50. Dong, Y.; Yang, Q.; Jia, S.; Qiao, C. Effects of high pressure on the accumulation of trehalose and glutathione in the *Saccharomyces cerevisiae* cells. *Biochem. Eng. J.* **2007**, *37*, 226–230. [CrossRef]
- 51. Radhakrishnan, V.S. Silver nanoparticles induced alterations in multiple cellular targets, which are critical for drug susceptibilities and pathogenicity in fungal pathogen (*Candida albicans*). *Int. J. Nanomed.* **2018**, *13*, 2647–2663. [CrossRef]
- 52. Liang, S.X.T.; Wong, L.S.; Lim, Y.M.; Lee, P.F.; Djearamane, S. Effects of zinc oxide nanoparticles on *Streptococcus pyogenes*. South Afr. J. Chem. Eng. 2020, 34, 63–71. [CrossRef]
- 53. Dhanasegaran, K.; Djearamane, S.; Liang, S.X.T.; Wong, L.S.; Kasivelu, G.; Lee, P.F.; Lim, Y.M. Antibacterial properties of zinc oxide nanoparticles on *Pseudomonas aeruginosa* (ATCC 27853). *Sci. Iran.* **2022**, *28*, 3806–3815.
- 54. Eskandari, M.; Haghighi, N.; Ahmadi, V.; Haghighi, F.; Mohammadi, S.R. Growth and investigation of antifungal properties of ZnO nanorod arrays on the glass. *Phys. B Condens. Matter* **2011**, *406*, 112–114. [CrossRef]
- 55. Sharma, R.K.; Ghose, R. Synthesis of zinc oxide nanoparticles by homogeneous precipitation method and its application in antifungal activity against *Candida albicans*. *Ceram. Int.* **2014**, *41*, 967–975. [CrossRef]

Coatings 2022, 12, 1988 12 of 12

56. Kasemets, K.; Ivask, A.; Dubourguier, H.C.; Kahru, A. Toxicity of nanoparticles of ZnO, CuO and TiO₂ to yeast *Saccharomyces cerevisiae*. *Toxicol*. *In Vitro* **2009**, 23, 1116–1122. [CrossRef] [PubMed]

- 57. Galván Márquez, I.; Ghiyasvand, M.; Massarsky, A.; Babu, M.; Samanfar, B.; Omidi, K.; Golshani, A. Zinc oxide and silver nanoparticles toxicity in the baker's yeast, *Saccharomyces cerevisiae*. *PLoS ONE* **2018**, *13*, e0193111. [CrossRef]
- 58. Abdul, A.T.; Ali, A.F. Effect of zinc oxide nanoparticles on *candida albicans* of human saliva (in vitro study). *Int. J. Res. Dev. Pharm. Life Sci.* **2015**, *4*, 1892–1900.
- 59. Xia, T.; Kovochich, M.; Liong, M.; Madler, L.; Gilbert, B.; Shi, H.; Nel, A.E. Comparison of the mechanism of toxicity of zinc oxide and cerium oxide nanoparticles based on dissolution and oxidative stress properties. *ACS Nano* **2008**, *2*, 2121–2134. [CrossRef]
- 60. Zhang, H.; Chen, G. Potent antibacterial activities of Ag/TiO₂ nanocomposite powders synthesized by aone-potsol–gel method. *Environ. Sci. Technol.* **2009**, 43, 2905–2910. [CrossRef]